Design and Performance of a Planar Array Infrared Spectrograph that Operates in the 3400 to 2000 cm^{-1} Region

DOUGLAS L. ELMORE*, MEI-WEI TSAO, SIMON FRISK, D. BRUCE CHASE, and JOHN F. RABOLT†

University of Delaware, Department of Materials Science and Engineering, Newark, Delaware 19716-3106 (D.L.E., M.-W.T., S.F., D.B.C., J.F.R.); and Central Research and Development, DuPont Experimental Station, Wilmington, Delaware 19880-0328 (D.B.C.)

A prototype, no-moving-parts, plane array infrared spectrograph (PA-IR) capable of routine spectral acquisition in the 3400 to 2000 cm^{-1} region has been constructed. The instrument includes a continuous source, Czerney–Turner type monochromator system and an infrared camera that incorporates a 320 × 256 pixel InSb focal plane array detector cooled with liquid nitrogen. PA-IR spectra (~3400 to 2550 cm^{-1}) of polystyrene (PS) and poly(ethylene naphthalate) (PEN) films have been obtained at a resolution of ~8 cm^{-1} with excellent signal-to-noise ratios (SNR). Peak-to-peak noise levels of ~1×10^{-3} absorbance units are observed for single acquisition spectra with 1.5 ms integration times and 17 ms total acquisition times. Integration times as low as 10 μs are possible (with good SNR); however, data acquisition is limited by the frame rate (60 frames/s) of the software acquisition package currently used. In this work, an apertured image of the source is displayed over ~20 rows of the array and the expected square root improvement in SNR is observed when multiple rows and/or frames are averaged. We have also shown that a square root improvement in SNR continues to occur with further signal averaging, providing noise levels as low as 1.5×10^{-5} absorbance units. Several additional advantages and options associated with the PA-IR method are discussed, including time-resolved spectroscopy, real-time monitoring, and spectroscopic mapping.

Index Headings: **Planar array infrared spectrograph; Focal plane array; InSb; Instrumentation design; Time-resolved spectroscopy; Real-time monitoring; Infrared imaging.**

INTRODUCTION

For a generation of spectroscopists, Fourier transform infrared (FT-IR) spectrometers have defined the instrumental state of the art.[1] With these instruments, fast, sensitive measurements can be made with extremely precise frequencies. Unfortunately, the moving mirror mechanism in a traditional interferometer ultimately limits the data acquisition speed and the ruggedness of the spectrometer. In order to reduce these limitations, instrumental designs with no moving parts have been considered as alternatives to fast scan FT-IR spectrometers but with a limited amount of applicability. One of these employed an all-fiber-optic interferometer with temperature driven modulations.[2] In this study the authors described a prototype all-fiber-optic FT interferometer that operated in the near-infrared region, and they discussed the possibility of extending the design to the mid-infrared region. Other researchers have utilized a multi-channel detector in a spectrographic configuration.[3–6]

In the last decade, the quality and quantity of commercially available infrared linear array and focal plane array (FPA) detectors has improved significantly with a concurrent drop in price. Infrared FPA detectors, which have been used in infrared cameras and sensors for some time, have recently been utilized in Fourier transform infrared (FT-IR) imaging systems.[7,8] This FT-IR and FPA based imaging technique has gained considerable popularity in determining the spatial distribution of different chemical species in a variety of materials.[8–13]

The idea of a linear array infrared spectrometer was first considered by Richardson et al.[3] In this work the researchers described a functioning prototype that utilized a 32 element InSb linear array. The instrument produced spectra with a nominal resolution of 32 cm^{-1} and a root mean square (rms) noise level of ~0.01 absorbance units in 4 μs for the region between 2650 and 2400 cm^{-1}. The authors indicated that spectra with resolution as high as 16 cm^{-1} could be collected with a two-fold decrease in the SNR. In a second study, Richardson et al.[4] re-examined the potential of this instrument for collection of time-resolved spectra in the microsecond time domain. They demonstrated that the spectrograph could collect infrared spectra with a spectral coverage of ~250 cm^{-1} every 16 μs at a nominal resolution of 32 cm^{-1} with an rms noise of ~0.002 absorbance units.

In 1994, Hamm et al.[5] reported an ultrafast infrared spectroscopic method that utilized a mercury cadmium tellurium (MCT) linear array detector, and in 1997, Heilweil et al.[6] reported an ultrafast method that utilized an InSb FPA detector. In both studies, infrared probe and reference pulses were generated by the difference-frequency mixing of femtosecond laser pulses and dispersed by a monochromator onto an FPA. The method described by Hamm et al.[5] featured a spectral range of 65 cm^{-1}, a resolution that varied between 3 and 10 cm^{-1}, and an rms

Received 29 October 2001; accepted 12 November 2001.

* Address as of 25 February 2002: Memphis Analytical Technology Center, Cargill, Cordova, Tennessee 38016.

† Author to whom correspondence should be sent.

0003-7028/02/5602-0145$2.00/0

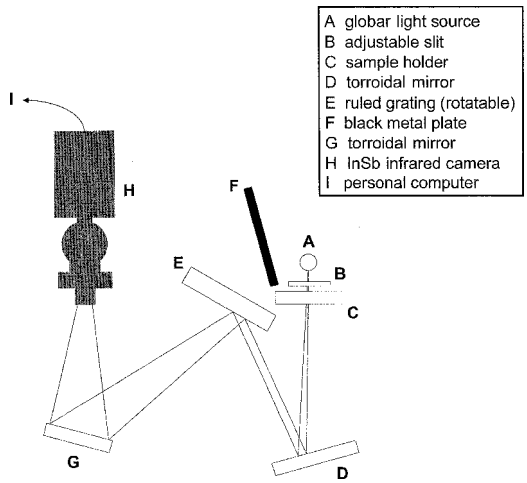

FIG. 1. Experimental arrangement of components in the PA-IR spectrograph.

noise level as low as 4×10^{-5} absorbance units for a five minute acquisition time. The Heilweil study[6] featured a spectral range ≤ 400 cm^{-1}, 15-cm^{-1} resolution, and an rms noise level of 3×10^{-4} absorbance units for a 17 minute acquisition time (2×10^4 total shots).

In this paper we describe a planar array infrared (PA-IR) spectrograph capable of routine spectral acquisition in the 3400 to 2000 cm^{-1} region using an InSb FPA and a continuous broadband infrared source.[14] Our current instrumental setup features a no-moving-parts configuration (during spectral acquisition), a frequency range of ~850 cm^{-1} (tunable between ~3400 to 2000 cm^{-1}), a resolution of ~8 cm^{-1}, and a noise level as low as $\sim 1 \times 10^{-3}$ absorbance units for a single acquisition spectrum with an integration time of 1.5 ms and a total acquisition time of 17 ms.

EXPERIMENTAL

PA-IR Spectrograph. A block diagram of the PA-IR spectrograph is presented in Fig. 1. Broad band infrared radiation, produced by a globar, passes through an adjustable slit and a sample holder. After reflecting off a torroidal mirror, the radiation is diffracted by a ruled grating (rotatable), reflects off another torroidal mirror, is then collected (with f/2.3 condensing optics), and is focused onto an InSb 320 × 256 focal plane array (FPA) detector cooled with liquid nitrogen. Camera optics include a 3–5-μm band pass filter for noise reduction.

The spectrograph was constructed on a Newport (NRC) optical table without an operational vibration-isolation system. The globar used in this instrument was ~1.2 cm high, with a diameter of ~2 mm, and was driven by a regulated power supply. An adjustable slit (0–2 mm), set at ~0.3-mm width, was used to collect spectra at 1.5 ms integration times. The torroidal mirrors were silver-coated on the front surface and had a focal length of 10 cm. The ruled grating had 300 grooves/mm (SPEX, Edison, NJ) and a blaze wavelength of 4.0 μm. The FPA, with 30 × 30 μm pixels, is housed in the dewar of a Merlin™ InSb Laboratory Infrared Camera (Indigo Systems, Santa Barbara, CA). A frequency range of ~5 cm^{-1} illuminated each pixel. The optical configuration has not been optimized.

In an FPA infrared detector, the pixels vary in their individual response to photon energy. This situation is commonly referred to as ''non-uniformity''. To achieve a uniform image, a two-point (gain and off-set) non-uniformity correction of the FPA response was performed at the beginning of the study with a 1.5 ms integration time using ~75% of the camera's dynamic range. One-point non-uniformity corrections were performed prior to data acquisition. The two points were obtained from an anodized metal plate both at elevated and room temperature. The one-point correction was obtained solely with the metal plate at room temperature.

Raw spectral data files were collected and saved as 320 × 256 images (TIF) using Image-Pro Plus software (Media Cyberbnetics, Silver Spring, MD) and a personal computer with a 650 MHz processor and 256 Mbytes of RAM. The frame rate was 60 frames/s, limiting the minimum total acquisition time to 17 ms.

PA-IR Spectra. Ratioed spectra were calculated using Excel (Microsoft, Redmond, WA) and plotted using GRAMS/32 (Galactic Industries, Salam, NH). A dark background spectrum was obtained by blocking the beam path with a metal plate. The dark background was then subtracted from the sample and background single beams before they were ratioed to produce photometrically accurate spectra. Transmittance spectra were calculated using the following equation:

$$T = (I_s - I_{db})/(I_o - I_{db}) \quad (1)$$

where T represents transmittance. I_s represents the uncorrected sample intensity and is the measured intensity when a sample is placed in front of the slit. I_o represents the uncorrected background and is the measured intensity of the open beam path. I_{db} represents the dark background and is the measured intensity when a metal plate is placed in front of the slit. Absorbance spectra were calculated as $A = -\log(T)$. All the polystyrene (PS) and poly(ethylene naphthalate) (PEN) spectra presented in this work were obtained by averaging 64 single acquisition spectra. Each single acquisition spectrum was obtained from one pixel row of the FPA.

FT-IR Measurements. Infrared spectra were collected at 4, 8, and 16 cm^{-1} resolution with a Nexus 670 FT-IR Fourier transform infrared spectrometer (Thermo Nicolet Corp., Madison, WI) equipped with a DTGS detector. Each spectrum was collected with one scan, apodized with a medium Beer–Norton function, and Fourier transformed with one level of zero filling. Both the FT-IR and PA-IR spectra were interpolated using the 4-point spline algorithm in the GRAMS/32 software. Interpolation factors were chosen in each case to yield a spectral data point every ~0.5 cm^{-1}.

Frequency Calibration. Frequencies in the PA-IR spectra were calibrated using a method similar to that commonly employed in dispersive Raman spectroscopy. First an FT-IR spectrum of a 25-μm PEN film was acquired at 8 cm^{-1} resolution; then a PA-IR spectrum of the same sample was obtained under identical conditions. The peak maxima were determined in cm^{-1} (FT-IR) and pixel number (PA-IR) by simply choosing the most intense point in each band. The relationship between the cm^{-1} values and pixel numbers was then fitted with a polynomial, producing a frequency calibration function.

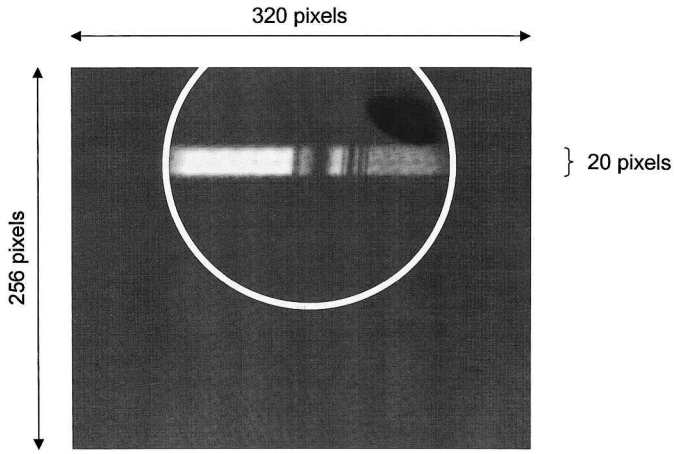

FIG. 2. PA-IR spectral image of PS.

Specifically, the calibration function was determined using eight peaks and a fourth-order polynomial. Frequency values with ≤ 0.2 cm^{-1} error were obtained with this method. It should be noted that more accurate frequency values can be determined by using a calibration sample that contains a large number of well-resolved peaks in the region of interest and by using a more precise method for determining peak position.

RESULTS AND DISCUSSION

Figure 2 shows a slit image dispersed across the FPA (spectral image) after a PS film was placed in the sample position of the PA-IR spectrograph described by Fig. 1. The light color indicates areas of high signal intensity, while the dark color indicates areas of low signal intensity corresponding to the strong spectral absorbances observed for PS in the ~3200 to 2800 cm^{-1} region. The spectral image is about 20 pixel rows high and about 200 pixels wide. The height of the image is determined by the height of the globar light source (the globar height is less than the slit height) and the monochromator optics.

The corresponding single beam spectrum of PS is presented in Fig. 3, spectrum ***B***. Also included in Fig. 3 is the single beam spectrum with no sample (***A***, the instrument line profile), the light path blocked in front of the sample holder (***C***, the dark background), and the light path blocked directly in front of the camera optics (***D***, camera background). Figure 4 shows the corresponding transmittance spectrum of PS with a useful frequency range of ~850 cm^{-1}.

Reviewing the image in Fig. 2, it appears that the frequency range is limited by the diameter of the final toroid mirror in the optical setup, i.e., only ~66% of the pixels are used along a given row of the array. Thus, it may be possible to expand the frequency range to ~1300 cm^{-1} (~50% increase) simply by replacing the existing mirror with one of larger diameter.

Also note in Fig. 2 that the spectral frequencies shift to larger pixel numbers when observing separate pixel rows from the bottom to the top of the spectral image. We believe that the problem probably exists because the optics are currently not optimized. In future work we will try to correct this problem by fine tuning the optical setup. If an unacceptable amount of frequency shifting is still apparent, individual frequency calibrations will be performed on each pixel row.

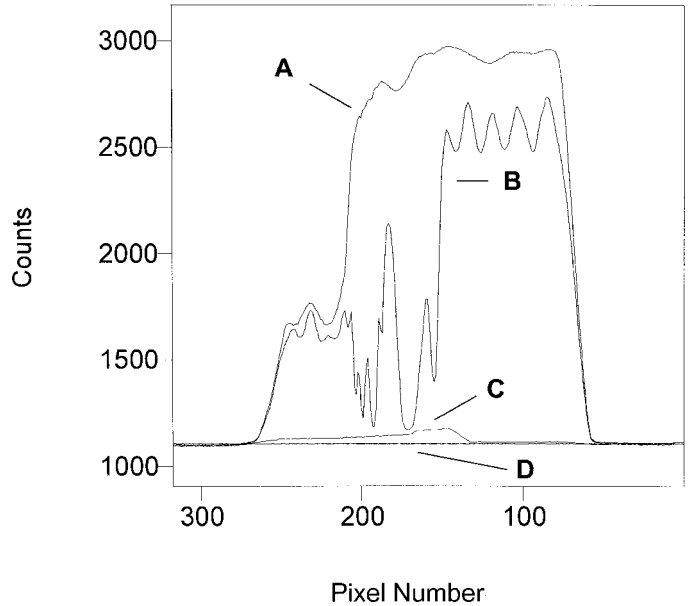

FIG. 3. PA-IR single beam spectrum of (***A***) the instrument line profile (background); (***B***) a single beam spectrum of a PS film; (***C***) the dark background; and (***D***) the camera background.

A PA-IR absorbance spectrum of PEN is presented in Fig. 5, spectrum ***A***, while FT-IR absorbance spectra of the same PEN sample are presented in spectra ***B–D***. The FT-IR spectra were collected at 4, 8, and 16 cm^{-1} resolution, respectively. Careful comparison of the PA-IR spectrum with the FT-IR spectra shows that the experimental resolution of the PA-IR spectrum is ~8 cm^{-1}, and the entire 850-cm^{-1}-wide spectral range is accurately represented.

PA-IR 100% lines differing only by the number of coadds are presented in Fig. 6, spectra ***A–C***. In spectrum ***A***, a 100% line is presented with a peak-to-peak noise

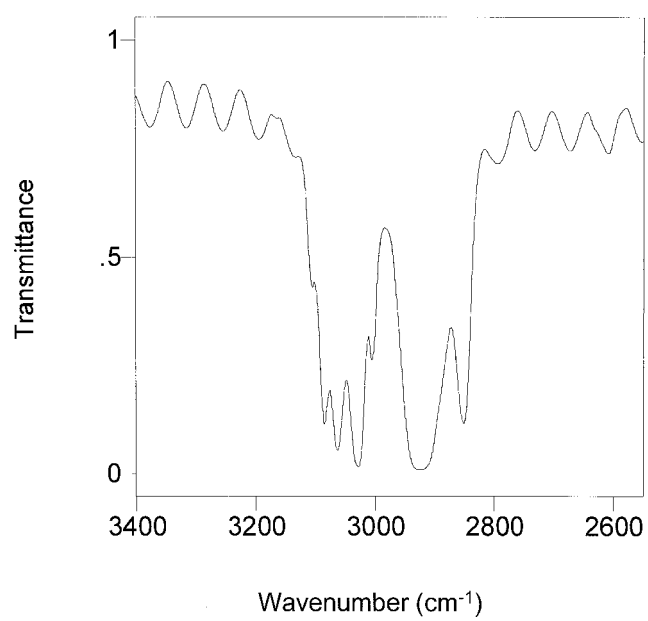

FIG. 4. PA-IR transmittance spectrum of PS.

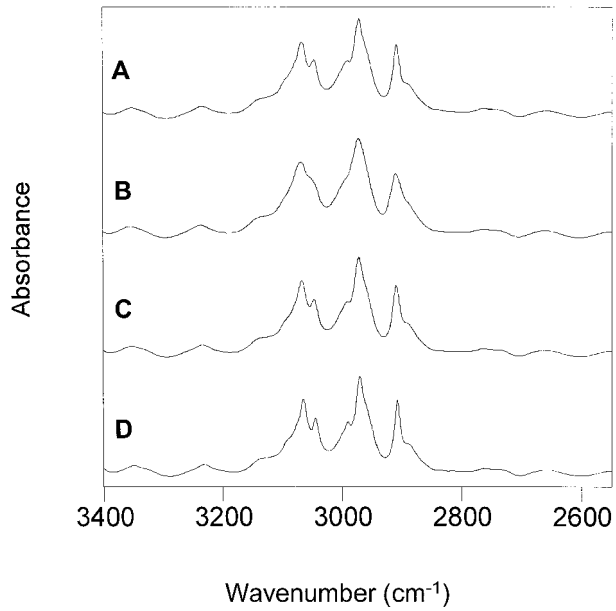

FIG. 5. (*A*) PA-IR absorbance spectrum of PEN. FT-IR absorbance spectra of the same PEN sample at (*B*) 16 cm^{-1}; (*C*) 8 cm^{-1}; and (*D*) 4 cm^{-1} resolution.

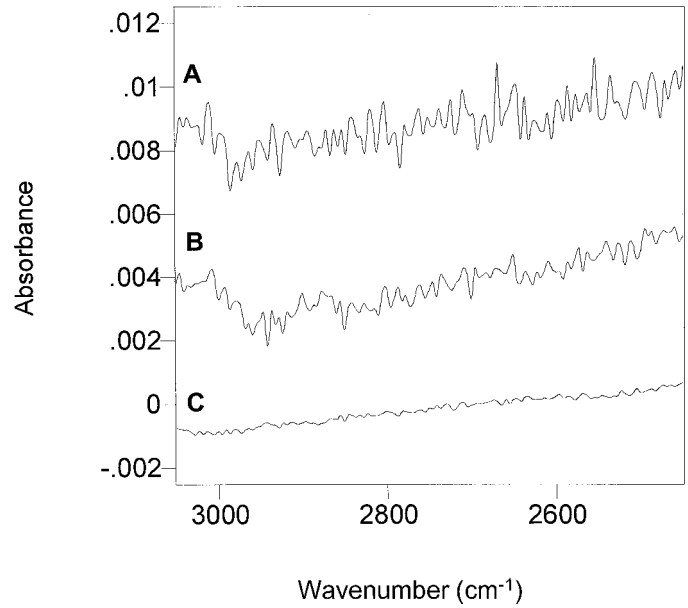

FIG. 6. PA-IR 100% lines differing only by the number of coadds. Single beams used to calculate the 100% lines were obtained from (*A*) one row of one frame, (*B*) nine rows of one frame, and (*C*) nine rows of 25 frames.

level of $\sim 2.7 \times 10^{-3}$ absorbance units that was obtained from one row of one frame (one coadd) collected with an integration time of 1.5 ms and a total acquisition time of 17 ms. In spectrum *B*, a 100% line is presented with a peak-to-peak noise level of $\sim 1.1 \times 10^{-3}$ absorbance units that was obtained from nine rows (nine coadds) of one frame collected with an integration time of 1.5 ms and a total acquisition time of 17 ms. In spectrum *C*, a 100% line is presented with a peak-to-peak noise level of $\sim 2.2 \times 10^{-4}$ absorbance units that was obtained from nine rows of 25 frames (225 coadds) collected with a total integration time of 38 ms and a total acquisition time of 417 ms.

When spectra *B* and *C* in Fig. 6 are compared, the expected square root improvement in SNR is observed. When spectra *A* and *B* are compared, a reduction in the noise level close to the expected improvement is observed. The small but apparent deviation from the expected square root improvement in SNR is observed because the single beams obtained from different rows have different intensities. If we take into account the varying single beam intensities, SNR improves as the square root of the number of coadds. This clearly demonstrates the advantage of multi-row and multi-frame averaging.

All the single acquisition spectra presented here were collected with a 1.5 ms integration time because a two-point non-uniformity correction of the FPA response was performed at the beginning of the study with this same integration time. However, it should be noted that the infrared light beam is attenuated and integration times as low as 50 μs could be obtained with similar SNR when no attenuation is applied. Noise levels associated with 10 μs integration times were about five times larger, since the amount of light striking the detector was $\sim 5\times$ less than the level that would saturate the detector. In the future, the amount of light available for these very short integration times could be increased by incorporating a collection mirror in the optical setup close to the infrared light source. Furthermore, it should be noted that integration times shorter than 10 μs should be possible by incorporating a detector with windowing capability (an option that our detector does not have). And in general, the system could be improved by modifying the optics to spread the spectral image over a larger area of the focal-plane.

Peak-to-peak noise levels as low as 1.5×10^{-5} absorbance units have been obtained with additional averaging of frames and rows. Figure 7, spectra *A*–*D*, show a series of 100% lines obtained with the PA-IR spectrograph utilizing a low voltage (1.5 V) IR source for future portable applications. In Fig. 7, spectrum *A*, a 100% line obtained

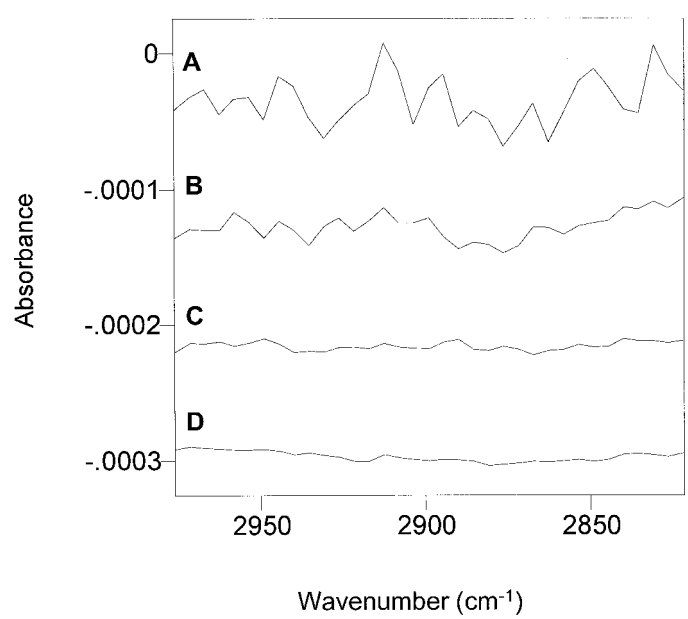

FIG. 7. PA-IR 100% lines using a low voltage IR source. (*A*) 4000 coadds; (*B*) 16 000 coadds; (*C*) 64 000 coadds; and (*D*) 256 000 coadds.

from 4000 coadds (one pixel row from 4000 frames) is shown that was collected with a total integration time of six seconds and a total acquisition time of 68 seconds. The peak-to-peak noise level of the baseline is $\sim 1.2 \times 10^{-4}$ absorbance units. In Fig. 7, spectrum ***B***, a 100% line obtained from 16 000 coadds (four pixel rows from 4000 frames) is shown that was collected with a total integration time of 25 seconds and a total acquisition time of five minutes. The peak-to-peak noise level of the baseline is $\sim 6.0 \times 10^{-5}$ absorbance units. In Fig. 7, spectrum ***C***, a 100% line obtained from 64 000 coadds (four pixel rows from 16 000 frames) is shown that was collected with a total integration time of 98 seconds and a total acquisition time of 18 minutes. The peak-to-peak noise level of the baseline is $\sim 3.0 \times 10^{-5}$ absorbance units. In Fig. 7, spectrum ***D***, a 100% line obtained from 256 000 coadds (16 pixel rows from 16 000 frames) is shown that was collected with a total integration time of 6.5 minutes and a total acquisition time of 73 minutes. The peak-to-peak noise level of the baseline is $\sim 1.5 \times 10^{-5}$ absorbance units. In Fig. 7, spectra ***A–D***, the number of coadds increases sequentially by a factor of four from figure to figure. When the 100% lines are compared, the expected two-fold SNR improvement is observed from spectrum to spectrum, demonstrating that signal averaging can be used to obtain noise levels as low as $\sim 1.5 \times 10^{-5}$. The absolute averaging limit, which is still unknown, will be determined and reported in future work.

Since the instrument employs an FPA detector, the PA-IR spectrograph provides several advantages and options including: (1) a multi-channel advantage; (2) the very short integration times ($\geq$10 μs); the response of InSb FPA detector is very fast and is therefore well suited for time-resolved spectroscopic measurements. While the frame rate currently restricts time-resolved measurements to the millisecond time domain, it is important to note that the FPA is capable of integration times as low as 10 μs and therefore can perform microsecond domain measurements if the frame rate is sufficiently increased; (3) no moving parts during data acquisition; the spectrograph is therefore well suited for portable configurations; (4) a very simple experimental setup; the setup is thus easily modified for different applications; and (5) pixel binning options. Some of these options are considered in the following discussion.

Due to the large number of pixel rows available in the FPA, it is possible to illuminate the FPA with two or more separate and independent spectral images. For example, one spectral image located near the top of the pixel array could correspond to a frequency range of 3100–2800 cm^{-1} (CH_2 stretching region), while another spectral image located near the bottom of the array could correspond to the 2300–2000 cm^{-1} frequency range (CD_2 stretching region).

Real-time background corrections can be performed by obtaining sample and background single beams from different portions of the same spectral image. One simple way to accomplish this is to lower a sample into the beam path until spectral absorbances are observed in the upper portion of the spectral image. Some of the top rows of the image are then used to obtain sample single beams while some of the bottom rows are used to obtain background single beams. It should be noted that single beams taken from different rows have slightly different profiles; therefore, some method of compensation is required in the data processing scheme.

Technically, individual single beams obtained from the FPA are spatially resolved along the vertical length of the slit, i.e., the light passing through the very top of the slit corresponds to the top pixel row of the spectral image, while the light passing through the very bottom of the slit corresponds to the bottom row of the spectral image. By stepping the sample across the slit and systematically collecting spectra it is possible to spectroscopically and spatially map the sample.

CONCLUSION

A PA-IR spectrograph was described that produces high quality infrared spectra. The spectrograph provides fast measurements at high sensitivity and is therefore well suited for time-resolved applications (currently in the millisecond domain and potentially in the microsecond domain). The inherent ruggedness of the spectrograph is well suited for portable configurations, while the simple experimental arrangement allows modifications to easily be made for different sample applications. Some of the applications currently being pursued include time-resolved spectroscopy of polymer films, real-time monitoring, transmission and reflection spectroscopy of thin films, and the construction of a miniaturized portable spectrograph. In the latter application, we are exploring the use of an uncooled microbolometer FPA and a low voltage (1.5 V) infrared source to construct a portable spectrograph for monitoring dangerous gases.

ACKNOWLEDGMENTS

We would like to acknowledge support by the National Science Foundation (DMR 9812088 and DMR 9975756) and the Department of Energy PAIR program.

1. P. R. Griffiths and J. A. de Haseth, *Fourier Transform Infrared Spectrometry* (John Wiley and Sons, New York, 1986), 1st ed.
2. M. Stelzle, J. Tuchtenhagen, and J. F. Rabolt, Measurement Sci. Technol. **7,** 1619 (1996).
3. H. H. Richardson, V. W. Pabst, and J. A. Butcher, Appl. Spectrosc. **44,** 822 (1990).
4. S. M. Alawi, T. Krug, and H. H. Richardson, Appl. Spectrosc. **47,** 1626 (1993).
5. P. Hamm, S. Wiemann, M. Zurek, and W. Zinth, Opt. Lett. **19,** 1642 (1994).
6. S. M. Arrivo, V. D. Kleiman, T. P. Dougherty, and E. J. Heilweil, Opt. Lett. **22,** 1488 (1997).
7. E. N. Lewis, P. J. Treado, R. C. Reeder, G. M. Story, A. E. Dowrey, C. Marcott, and I. W. Levin, Anal. Chem. **67,** 3377 (1995).
8. E. N. Lewis, A. M. Gorbach, C. Marcott, and I. W. Levin, Appl. Spectrosc. **50,** 263 (1996).
9. J. L. Koenig, S. Q. Wang, and R. Bhargava, Anal. Chem. **73,** 360A (2001).
10. C. M. Snively and J. L. Koenig, Appl. Spectrosc. **53,** 170 (1999).
11. P. Colarusso, L. H. Kidder, I. W. Levin, J. C. Fraser, J. F. Arens, and E. N. Lewis, Appl. Spectrosc. **52,** 106A (1998).
12. C. D. Tran, Fresenius' J. Anal. Chem. **369,** 313 (2001).
13. C. Marcott, R. C. Reeder, J. A. Sweat, D. D. Panzer, and D. L. Wetzel, Vib. Spectrosc. **19,** 123 (1999).
14. Patent pending.